Characterization of the performance of 1–3 type piezocomposites for low-frequency applications

Q. M. Zhang, Wenwu Cao, H. Wang, and L. E. Cross
Materials Research Laboratory, The Pennsylvania State University, University Park, Pennsylvania 16802

(Received 20 April 1992; accepted for publication 15 October 1992)

In general, the piezoelectric ceramic and polymer in a 1–3 type composite will have different deformations when subjected to an external field. How each component deforms, to a large extent, determines the performance of the composite. Based on the force equilibrium condition, an elastic model is introduced to analyze the strain profiles of these composites, and the theoretical results are in quantitative agreement with the strain profiles measured on several composites using a double beam ultradilatometer. The results obtained provide quantitative information on how various parameters in a composite affect the performance of the composite. Furthermore, a scheme is proposed for evaluating the strain profile of a 1–3 type composite under a hydrostatic pressure using a double beam dilatometer.

I. INTRODUCTION

A variety of piezoelectric composite materials can be formed by combining a piezoelectric ceramic with a polymer phase. Among them, the piezoelectric 1–3 composite has attracted a great deal of attention and been used widely.[1–3] A typical configuration of 1–3 type composites is illustrated in Fig. 1. In the composites, piezoelectric ceramics, usually lead zirconia titanate (PZT) ceramics, play the active role of energy conversion between the mechanical energy and electric energy, while the polymer phase acts as a passive medium, which transfers the mechanical energy between the piezoelectric ceramic and the surrounding with which the composite interacts. The disparity in the physical properties between the two constituent phases and different roles they play in a composite make it possible to fine tailor the material properties of a composite to meet different requirements of specific application.[4–7]

There are two major areas where 1–3 composites have been widely used: underwater hydrophone application and ultrasonic actuators and sensors for medical diagnostic devices.[1–4] The former is operated at frequencies below 40 kHz while the latter are operated at a MHz frequency range. As can be seen from Fig. 1, in making a 1–3 composite, several parameters can be varied: the elastic properties of the polymer phase, the shape, and the aspect ratio of the PZT rods, the spacing between the rods, the volume content, and the arrangement of the PZT rods in the composite. The intention of this paper is to provide some understanding of how these design parameters affect the performance of the composites for low-frequency applications. To achieve that, a new model is introduced that treats the composites beyond the earlier equal-strain model.[2,8,9]

When a 1–3 composite is subjected to an electric field or a stress field, a strain field will be induced in the sample. Due to the large difference in the elastic and piezoelectric properties, in general, the two components will have different strain levels and the strain in each component will not be uniform. This strain profile is determined by the parameters listed in the preceding paragraph and determines how effectively the two components in a composite couple to each other. The strain profile of a composite under an electric field can be mapped out using a double beam ultradilatometer, as will be shown in this paper.[10] However, it may not be measured easily when the composite is subjected to a stress field. In this paper, we will show that the strain profile measured on a composite under an electric field can be used to describe the deformation of the composite under a uniaxial or a hydrostatic stress.

The basic elastic coupling mechanism between the two components in the 2–2 piezoelectric composite is similar to that of the 1–3 composite. Although this structure is not widely used, the mathematical analysis on the performance of the composite is much simpler and the results obtained can also be applied to the 1–3 composite. Hence, in this paper, we will first discuss the performance of 2–2 composites (Sec. II). In Sec. III, 1–3 composites will be analyzed in the dilute limit. In Sec. IV, the results obtained in Sec. III will be applied to 1–3 composites beyond the dilute limit.

II. 2–2 COMPOSITE

In a 2–2 composite, the PZT plates and polymer are arranged in a parallel manner, as schematically drawn in Fig. 2(a). Assuming the sample dimension in the y direction is much larger than the sample thickness L and the spacing d between the neighboring PZT plates, a 2–2 composite can be modeled as a one-dimensional system. When there is a strain change S_3 in PZT plates, for example, due to an electric field on the composite, there will be a corresponding change in the strain profile of the polymer phase. Denoting $u(x)$ the surface displacement of the polymer phase in the z direction, the longitudinal strain S_3 in the z direction of the polymer phase is $2u(x)/L$, where L is the sample thickness. As a result of the strain gradient $u(x)$, a shear force $\mu L\, \partial^2 u(x)/4\, \partial x^2$ will be induced in the z direction, where μ is the shear modulus of the polymer. Under the static condition, this shear force will be balanced by the restoring force $2Yu(x)/L$ in the polymer, that is

 0021-8979/93/031403-08$06.00

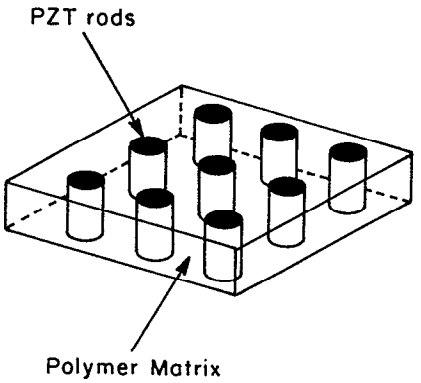

FIG. 1. Schematical drawing of a 1–3 PZT–polymer composite, where PZT rods are embedded in a polymer matrix.

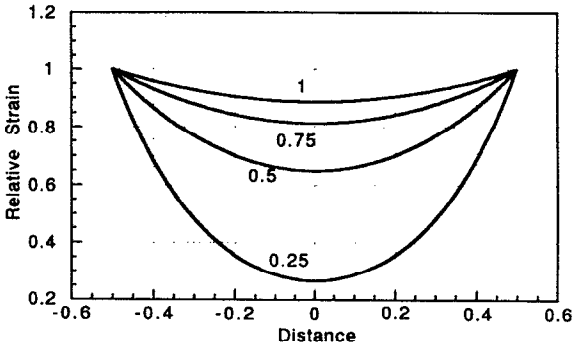

FIG. 3. The strain profile for the polymer between two PZT plates [from Eq. (1.3)]. The parameter shown in the figure for each curve is $\xi = L/(2\sqrt{2Y/\mu})$. In the figure, the gap width d is 1 mm.

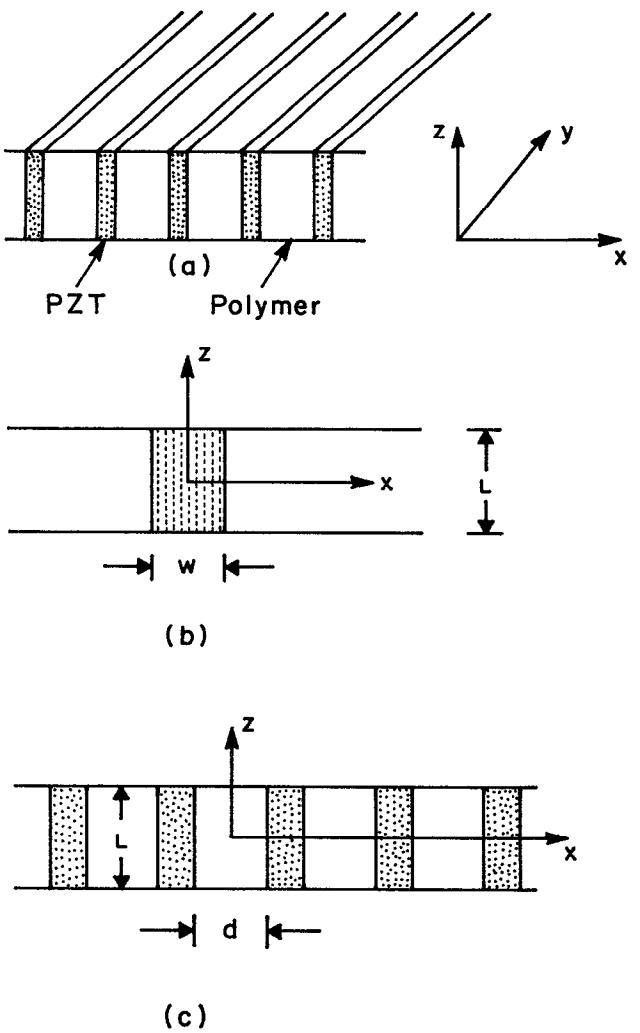

FIG. 2. (a) A schematical drawing of a 2–2 composite, where the hatched plates are PZT; (b) the coordinate system for a 2–2 composite with a single PZT plate; and (c) the coordinate system for Eq. (1.3).

$$\frac{\mu L}{4}\frac{\partial^2 u(x)}{\partial x^2}=\frac{2Y}{L}u(x), \tag{1.1}$$

where Y is the Young's modulus of the polymer. The details of the derivation of Eq. (1.1) will be presented in a separate paper.[11] The solution to Eq. (1.1) is

$$2u(x)/L=A\exp(2x\sqrt{2Y/\mu}/L)+B,$$

where A and B are integration constants. For the case when there is only one PZT plate in the composite, as shown in Fig. 2(b), the longitudinal strain S_3 of the polymer phase is

$$\left(\frac{2u}{L}\right)=\left(\frac{2u}{L}\right)_0\exp\left[-\left(x-\frac{w}{2}\right)\frac{2\sqrt{2Y/\mu}}{L}\right]\quad\left(x>\frac{w}{2}\right) \tag{1.2}$$

and

$$\left(\frac{2u}{L}\right)=\left(\frac{2u}{L}\right)_0\exp\left[\left(x+\frac{w}{2}\right)\frac{2\sqrt{2Y/\mu}}{L}\right]\quad(x<-w/2),$$

where w is the PZT plate width and $2(u/L)_0$ is the strain at the PZT–polymer interface. Equation (1.2) shows that the strain in the polymer phase decays exponentially with a characteristic length $\xi = L/(2\sqrt{2Y/\mu})$ as the polymer phase moves away from the PZT plate.

For a 2–2 composite as depicted in Fig. 2(c), the solution to Eq. (1.1) is

$$\left(\frac{2u}{L}\right)=\left(\frac{2u}{L}\right)_0\cosh\left(\frac{2x\sqrt{2Y/\mu}}{L}\right)\operatorname{sech}\left(\frac{d\sqrt{2Y/\mu}}{L}\right), \tag{1.3}$$

where d is the gap width between the two PZT plates. Equation (1.3) describes the strain profile in the polymer between the two neighboring PZT plates. In Fig. 3, we plot the strain profile of the polymer phase calculated from Eq. (1.3) for $L=4.7$ mm ($\xi=1$), 3.5 mm ($\xi=0.75$), 2.3 mm ($\xi=0.5$), and 1.2 mm ($\xi=0.25$) for the gap width $d=1$ mm. In the calculation, $Y=4.7\times10^9$ N/m^2 and $\mu=1.7\times10^9$ N/m^2, the elastic constants for spurs epoxy were used. The figure shows a strong dependence of induced strain profile in the polymer phase on the sample thickness.

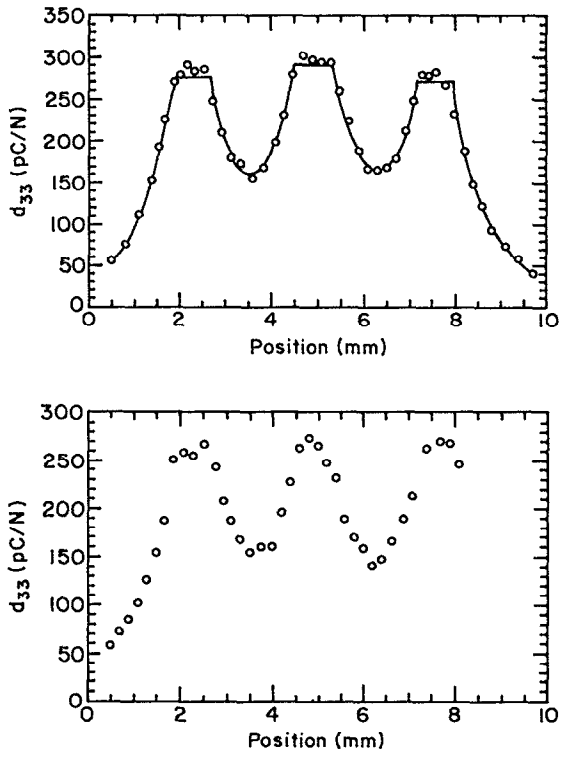

FIG. 4. (a) Strain profile for the 2–2 composite made of PZT-5A and spurs epoxy with thickness $L=4.5$ mm. The sample is driven electrically at 200 Hz, circles are the data points and the solid lines are the fitting. (b) Strain profile for the 2–2 composite measured at 40 kHz.

From the figure, one can make the following observations: in this one-dimensional structure, as the sample thickness approaches that of the gap width, induced strain in the gap center of the polymer phase approaches zero; On the other hand, for $L/d=5$, the strain nonuniformity in the polymer phase is less than 10% and the equal-strain model can be used to calculate the effective material properties without introducing significant errors. Equations (1.2) and (1.3) also reveal that the elastic properties of the polymer phase have a significant effect on the strain profile. By reducing Y or increasing μ, one can greatly increase the elastic coupling between the two components.

To compare with the theoretical results, several 2–2 composites were made using PZT-5A (PZT-5A and PZT-5H are trademarks of Vernitro Corp. for their PZT products) plates and spurs epoxy. The strain profile of the sample was measured along a path parallel to the x axis using the double beam laser interferometer when the sample was driven electrically. Shown in Fig. 4(a) is the result of one of the scans thus obtained. The solid line in the figure is the theoretical fitting using Eq. (1.3) for the polymer regions between the PZT plates and Eq. (1.2) for the polymer regions at the two edges of the sample. Clearly, the theoretical curve describes the data quite well. The fitting yields the ratio of $Y/\mu=3.35$ for spurs epoxy, which is larger than the true value of $Y/\mu(=2.76)$. We believe that this is due to the fact that in Eq. (1.1), the effect of the stress in the x and y directions is not included. Further work will be conducted to incorporate the lateral stress effect in the constitutive equations.

Equation (1.1) can be modified to account for the situation when a composite is subjected to a low-frequency driving field (either a stress field or an electric field). By low frequency, we mean that the frequency is at least five times smaller than the first thickness resonance frequency. Under this circumstance, the longitudinal strain in the sample can be approximated as uniform and Eq. (1.1) can be rewritten as

$$\frac{\mu L}{4}\frac{\partial^2 u}{\partial x^2}=\frac{2Y}{L}u+\frac{\rho L}{4}\frac{\partial^2 u}{\partial t^2}, \tag{1.4}$$

to include the time-dependent effect. In Eq. (1.4), ρ is the polymer density. For a sinusoidal strain $u=u(x)\exp(i\omega t)$, where ω is the angular frequency of the driving field, Eq. (1.4) becomes

$$\frac{\mu L}{4}\frac{\partial^2 u}{\partial x^2}=\left(\frac{2Y}{L}-\frac{\rho L\omega^2}{4}\right)u. \tag{1.5}$$

It is easy to realize that as long as the quantity $(2Y/L^2-\rho\omega^2/4)>0$, the solution to Eq. (1.5) is the same as that of Eq. (1.1). The strain profile in the polymer region is still described by Eqs. (1.2) and (1.3), except the characteristic decay length ξ becomes $\xi=L/[2\sqrt{2(Y-\rho\omega^2L^2/8)/\mu}]$. In all the practical cases, the change in ξ is very small. For instance, the change of ξ is about 2% when ω varies from 0 to 40 kHz for the 2–2 composite used here. To verify this, the strain profile of the 2–2 composite was measured at higher frequency (40 kHz) using the laser dilatometer. The data is shown in Fig. 4(b) and the strain profile is almost identical to that measured at 200 Hz [Fig. 4(a)]. The experimental as well as theoretical results both indicate that the polymer strain profile will not change significantly in this low-frequency region.

We now discuss the situation when the composite is subjected to a uniaxial stress T in the z direction. The force balance condition yields

$$T+\left(\frac{\mu L}{4}\right)\frac{\partial^2 u}{\partial x^2}=\frac{2Yu}{L}. \tag{1.6}$$

By making the variable substitution, $v=u-LT/(2Y)$, Eq. (1.6) becomes identical to Eq. (1.1). Hence the solution to Eq. (1.6) for the polymer strain profile between two PZT plates is

$$\left(\frac{2u}{L}\right)=A\cosh\left(\frac{-2x\sqrt{2Y/\mu}}{L}\right)+\frac{T}{Y}, \tag{1.7}$$

where $A=[(2u/L)_0-T/Y]\mathrm{sech}(-d\sqrt{2Y/\mu}/L)$, $(2u/L)_0$ is the strain at the PZT–polymer interface, and d is the gap width of the polymer phase between the two PZT plates.

Comparison of Eq. (1.3), which is the polymer strain profile induced by the PZT plates when the composite is driven electrically, with Eq. (1.7), which is the strain profile of the polymer phase when a uniaxial stress is applied on the composite, yields that except for the prefactor and a constant term, the functional forms of the two cases are the

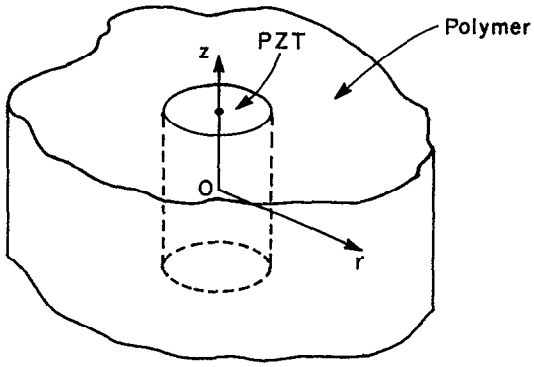

FIG. 5. 1–3 composite in the dilute limit.

same. As will be shown later in the paper, a similar conclusion is also true for the strain profile of a composite under a hydrostatic stress. This link between the two cases provides a convenient way for evaluating composites for hydrophone applications.

III. 1–3 COMPOSITE IN THE DILUTE LIMIT

In the dilute limit, the performance of a 1–3 composite can be modeled as that of a single PZT rod embeded in an infinitely extended polymer matrix, as schematically drawn in Fig. 5. From the symmetry of the problem, a cylindrical coordinate system is chosen with the z and r directions along the axis of the PZT rod and the radial direction, respectively. Similar to the situation for Eq. (1.1), the equation that describes the equilibrium condition of the polymer phase when the composite is driven electrically is

$$\frac{\mu L}{4}\left(\frac{\partial^2 u}{\partial r^2}+\frac{\partial u}{r\,\partial r}\right)=\frac{2Yu}{L}. \tag{2.1}$$

The meaning of each term in Eq. (2.1) is the same as that in Eq. (1.1). Equation (2.1) can be transformed to the zeroth-order Bessel equation of the imaginary argument. The solution that satisfies the boundary condition $r\to\infty$, $u/L\to 0$, is the imaginary argument zeroth-order Hankel function $K_0(\rho)$, where $\rho = 2r\sqrt{2Y/\mu}/L$. When the strain in the polymer phase is induced by the PZT rod, the solution to Eq. (2.1) is

$$(2u/L)=(2u/L)_0 K_0(\rho)/K_0(a/\xi), \tag{2.2}$$

where $(2u/L)_0$ is the strain at the PZT rod–polymer interface, a is the radius of the PZT rod, and $\xi = L/(2\sqrt{2Y/\mu})$.

It is interesting to compare the strain profile of the polymer phase in the 2–2 composite with that in the 1–3 composite. Shown in Fig. 6(a) are the strain profiles calculated from Eq. (2.2) (single PZT rod 1–3 composite) and from Eq. (1.2) (single PZT plate 2–2 composite). Apparently, the strain decay in the polymer phase in a 1–3 composite is much faster than that in a 2–2 composite. Besides that, there is an additional difference between the two cases: the decay in the polymer phase for a 1–3 composite also depends on the PZT rod diameter $2a$, while in

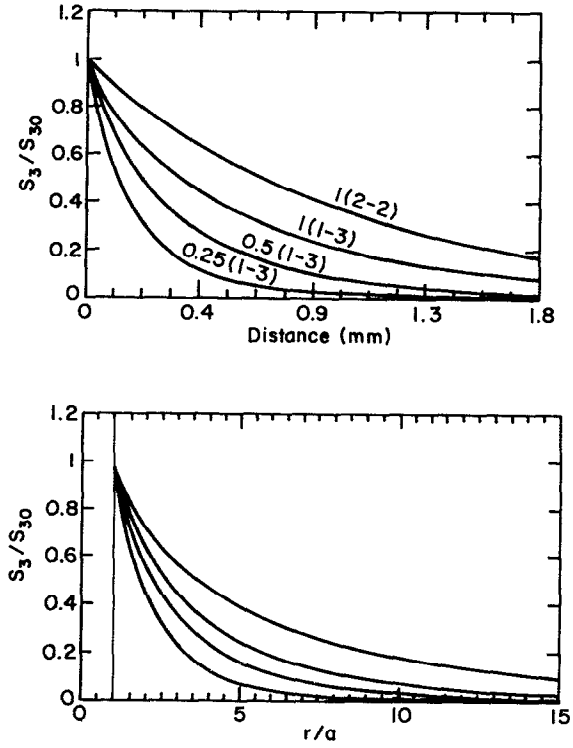

FIG. 6. (a) Decay of the strain in the polymer phase for (from the top to the bottom) a 2–2 composite [Eq. (1.2)] with $\xi=1$, a single rod 1–3 composite with $\xi=1$, $\xi=0.5$, and $\xi=0.25$, where $\xi = L/(2\sqrt{2Y/\mu})$. In the 1–3 composite, the PZT rod radius is 0.3 mm. The strain S_3 in the polymer phase is normalized to that of PZT rod S_{30}. The abscissa is the distance from the polymer–PZT interface. (b) The dependence of the strain in the polymer phase on the radius of a PZT rod in a 1–3 composite in the dilute limit. From the top to the bottom: $a=0.1$, 0.2, 0.3, 0.5 mm. In all the curves, $\xi=1$. r is distance defined in Fig. 5.

a 2–2 composite, it is independent of the PZT plate width. To illustrate this, in Fig. 6(b), the strain profiles in the polymer phase for PZT rod radius $a=0.1$, 0.2, 0.3, 0.5 mm are plotted, where $\xi=1$ and $(2u/L)_0=1$ are assumed for all the cases. Therefore, both the elastic properties of the polymer phase and the aspect ratio of the PZT rod are important parameters in determining the performance of 1–3 composites.[8,12]

Shown in Fig. 7 is the strain profile measured on a 1–3 composite made of a single PZT tube embeded in spurs epoxy matrix. The strain profile was mapped out using the double beam ultradilatometer when the sample was driven electrically at 200 Hz. The solid line in the figure is $K_0(r/\xi)$, the strain profile predicted theoretically. The only adjustable parameter in the fitting is ξ, and the theoretically calculated curve agrees with the experimental data quite well. The fitting yields the ratio of $Y/\mu=3.35$ for the spurs epoxy used, which is the same as that measured in the 2–2 case. The consistency between the two measurements indicates that the model contains the essence of the elastic coupling between the two components in 1–3 type composites.

In what follows, the elastic coupling between the PZT rod and polymer will be analyzed using this model for the composite subjected to (a) an electric field E along the z

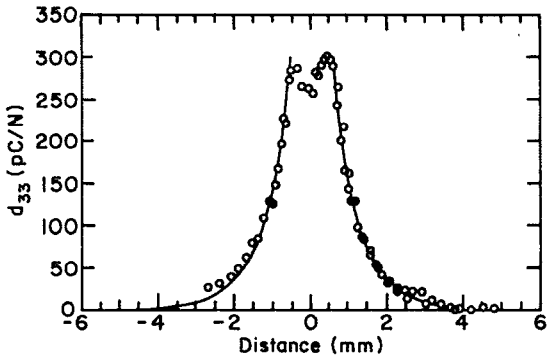

FIG. 7. The strain profile of a single tube 1–3 composite (tube o.d.=1.2 mm) measured at 200 Hz using the double beam ultradilatometer. The composite is made of PZT-5H tube and spurs epoxy. Solid lines are the fittings using Eq. (2.2) with only one adjustable parameter ξ ($\xi=1.15$ from the fitting). Sample thickness $L=4.5$ mm.

direction; (b) a uniaxial stress T along the z direction; and (c) a hydrostatic pressure. In all the cases, the poling direction of the PZT rod is in the z direction.

(a) when an electric field E is applied to the composite, from the constitutive equation, one can obtain the z component of the strain in the PZT rod $S_0=d_{33}E$ if there is no elastic coupling between the PZT rod and polymer. The effect of the polymer on the PZT rod is to add a mechanical load to it. In this situation, the strain in the polymer phase is described by Eq. (2.2). The stress transferred from the polymer to the PZT rod due to this strain field is

$$T=-Y(2u/L)_0F(a,\xi), \tag{2.3}$$

where $(2u/L)_0$ is the strain in the PZT rod after the polymer loading and

$$F(a,\xi)=\frac{2\xi K_1(a/\xi)}{a}, \tag{2.4}$$

where $\xi = L/(2\sqrt{2Y/\mu})$, a is the radius of the PZT rod, and $K_1(x)$ is the first-order modified Bessel function. The strain of the PZT rod due to this additional polymer loading is

$$\left(\frac{2u}{L}\right)_0=\frac{d_{33}E}{1+{}^cs_{33}YF(a,\xi)}, \tag{2.5}$$

where ${}^cs_{33}$ is the elastic compliance of PZT. Clearly, due to the polymer loading, the strain level of the PZT rod is smaller than $d_{33}E$. Using Eq. (2.5), one can calculate the strain reduction $(2u/L)_0/(d_{33}E)$ if ${}^cs_{33}Y$ and ξ are known. For a thin PZT rod (small a), even when the elastic compliance of the polymer is much larger than that of PZT, the reduction in the strain of the PZT rod can still be substantial.

In general cases, $d_{33}E$ can be replaced by S_0, the strain of the PZT rod without the polymer matrix. Hence the total stress on the PZT rod is

$$T=-\frac{YS_0F(a,\xi)}{1+{}^cs_{33}YF(a,\xi)}. \tag{2.6}$$

TABLE I. Stress amplification factor for 1–3 composites.

${}^cs_{33}Y$	0.02	0.1
a(mm)	γ	γ
0.1	31.4	9.0
0.2	8.3	7.6
0.5	7.1	4.8
1.0	3.6	3.0

A large stress would arise during the poling of a 1–3 composite since S_0 is relatively large as the PZT rods are poled, and this stress acts as a depoling field on the PZT rods in composites. For example, considering a composite made of a PZT-5H rod and spurs epoxy, taking $a=0.2$ mm, $L=5.2$ mm, $S_0=0.1\%$, $\xi=1$, ${}^cs_{33}Y=0.1$, and $Y=4.7\times10^9$ N/m^2, the stress on the PZT rod is 3.4×10^7 N/m^2.

(b) From the result of the preceding section, the strain profile of the polymer phase under a uniaxial stress T in the z direction is

$$(2u/L)=AK_0(r/\xi)+T/Y, \tag{2.7}$$

where $A=[(2u/L)_0-T/Y]/K_0(a/\xi)$, $(2u/L)_0$ is the strain of the PZT rod. When a composite is used in this situation, one major concern is how much the stress on the polymer will be transferred to the PZT rod. To calculate this quantity, we notice that without the elastic coupling to the PZT rod the strain in the polymer under the stress T is T/Y. By subtracting out this quantity from Eq. (2.7), one can obtain the change in the strain profile of the polymer phase due to the elastic coupling to the PZT rod. From this consideration, T_{tr}, the stress transferred from the polymer to the PZT rod is

$$T_{tr}=T\left\{\frac{1+F(a,\xi)}{1+({}^cs_{33}Y)F(a,\xi)}-1\right\}, \tag{2.8}$$

or in a more familiar language, the stress amplification factor γ due to the composite

$$\gamma=T_{total}/T=[1+F(a,\xi)]/[1+({}^cs_{33}Y)F(a,\xi)], \tag{2.9}$$

where $T_{total}=T+T_{tr}$ is the total stress applied to the PZT rod. In Table I, γ is calculated for composites with a different radius of the PZT rod and different elastic properties of the constituent phases ($\xi=1$). For a composite with a fixed volume percentage of PZT rods, the effective d_{33} of the composite is proportional to γ. Therefore, the result in Table I illustrates how the effective d_{33} of the composite changes as one varies the radius of PZT rods. Clearly, to increase the piezoelectric response of the composite, thin PZT rods should be used. The result in Table I also shows that the polymer self-loading (polymers with a large Young's modulus) will significantly reduce the amount of stress to be transferred to the PZT rod and result in a smaller γ.

In Eq. (2.9), as Y/μ approaches zero, $F(a,\xi)$ will approach the value of the equal-strain model and γ reaches its maximum value for a fixed ${}^cs_{33}Y$. Hence, to improve the

stress transfer in a composite, a polymer with a large μ and a small Y will be advantageous.

(c) In the hydrophone application, a 1–3 composite is subjected to a hydrostatic pressure. The stress on the composite will modify the equilibrium equation (2.1) of the polymer phase to

$$\left(\frac{2u}{L}\right)=s_{33}T_3+s_{31}T_1+s_{32}T_2+s_{33}\mu\,\frac{L}{4}\left[\frac{\partial^2 u}{\partial r^2}+\left(\frac{1}{r}\right)\frac{\partial u}{\partial r}\right]. \tag{2.10}$$

Making use of the relation $s_{31}=s_{32}=-\sigma s_{33}$, where σ is the Poisson's ratio of the polymer, $T_1=T_2=T_3=T$ in the hydrostatic condition, and $Y=1/s_{33}$, Eq. (2.10) can be rewritten as

$$Y\left(\frac{2u}{L}\right)=(1-2\sigma)T+\frac{\mu L}{4}\left[\frac{\partial^2 u}{\partial r^2}+\left(\frac{1}{r}\right)\frac{\partial u}{\partial r}\right]. \tag{2.11}$$

The solution to this equation is

$$\left(\frac{2u}{L}\right)=(1-2\sigma)\,\frac{T}{Y}+\left[\left(\frac{2u}{L}\right)_0-(1-2\sigma)\,\frac{T}{Y}\right]\frac{K_0(r/\xi)}{K_0(a/\xi)}. \tag{2.12}$$

The meaning of each quantity in Eq. (2.12) is the same as that in Eq. (2.7). Comparison between Eqs. (2.7) and (2.12) yields that the effect of hydrostatic pressure on a composite is to reduce the effective pressure on the polymer phase from T to $(1-2\sigma)T$. In the case of $\sigma=0.5$, this effective pressure becomes zero, a situation where the polymer becomes incompressible. On the other hand, Eq. (2.12) shows that the strain profile in the polymer phase is still described by the elastic constant ratio $2Y/\mu$, which is the same as that in the uniaxial stress situation. Hence, it is more appropriate to describe the reduction of the polymer strain level in the hydrostatic case as related to the reduction of the effective stress on its surface, rather than the change in the elastic constants of the material.

To find the total stress T_{total} exerted on the PZT rod, one has to calculate the strain of the PZT rod $(2u/L)_0$ in the composite under the hydrostatic pressure T. Using the reciprocal relation that the total force of the polymer phase on the PZT rod is equal in magnitude and opposite in sign to the total force of the PZT rod on the polymer phase, one can find T_{total},

$$T_{\text{total}}=T\,\frac{1+(1-2\sigma)F(a,\xi)-Y[{}^cs_h+(1-2\sigma){}^cs_{33}F(a,\xi)]}{1+{}^cs_{33}YF(a,\xi)}\times F(a,\xi), \tag{2.13}$$

where ${}^cs_h={}^cs_{33}+2{}^cs_{31}$ is the hydrostatic elastic compliance of the PZT rod, and a is the PZT rod radius. Hence, in the dilute limit, the hydrostatic piezoelectric constant d_h in the composite is related to the piezoelectric constant ${}^cd_{ij}$ of the PZT rod by the equation

TABLE II. Hydrostatic piezoelectric charge constant for 1–3 composites with a 5% PZT volume content. In the calculation ${}^cd_{33}=590$ pC/N and ${}^cd_h=45$ pC/N are used.

	$a=0.3$ mm		$a=0.5$ mm	
Y^cs_{33}	0.02	0.1	0.02	0.1
ξ	d_h (pC/N)			
1.0	106	55	60	39
0.5	51	34	24	19

$$d_h=\left[{}^cd_{33}\left(1+(1-2\sigma)F(a,\xi)-\frac{Y[{}^cs_h+(1-2\sigma){}^cs_{33}F(a,\xi)]F(a,\xi)}{1+{}^cs_{33}YF(a,\xi)}\right)+2{}^cd_{31}\right]v_0, \tag{2.14}$$

where v_0 is the volume fraction of PZT rods in the composite and ${}^cd_{33}$ and ${}^cd_{31}$ are the piezoelectric constants of PZT ceramics. Equation (2.14) is derived under the condition that the ceramic content in the composite is very low (dilute limit). Introducing Δ as the distance at which the polymer strain changes from $(2u/L)_0$ to $0.1(2u/L)_0$, we may define the criterion for the dilute limit in a 1–3 composite, that the distance between the two neighboring rods should be equal to or greater than $(2a+\Delta)$. For example, if the PZT rod radius is 0.25 mm, the dilute limit corresponds to about 5% or less PZT in a composite. Table II lists the d_h value calculated using Eq. (2.14) for composites with a 5% PZT rod of radius 0.3 mm and 0.5 mm. In the calculation, $\sigma=\frac{1}{3}$ is assumed for the polymer and $s_{31}=-\frac{1}{3}s_{33}$ is used for the PZT rod. The data indicate how d_h varies with PZT rod aspect ratio when the volume content of PZT is kept constant, and the effect of the polymer self-loading. The results are consistent with the existing experimental data.[8,12,13]

IV. 1–3 COMPOSITE BEYOND THE DILUTE LIMIT

When the volume content of PZT rods in a composite becomes higher, as in most practical cases, the dilute approximation is not adequate in calculating the stress transfer properties between the PZT rods and polymer matrix. For a 1–3 composite as schematically drawn in Fig. 1, to solve the exact solution for the strain profile in the composite under either an electric field or a stress field can be quite involved, albeit it is not impossible. To avoid this complication and as a first-order approximation, we assume the solution for a 1–3 composite is a linear superposition of the solution in the dilute limit. Normally, the radius of the PZT rod used in 1–3 composites ranges from 0.1 to 0.5 mm, and as has been shown in the preceding section, for thin PZT rods, the strain decays rapidly as the polymer phase moves away from the PZT rod. Hence, if the volume percentage of PZT in the composite is not very high ($<20\%$), one only needs to consider the effect of the nearest neighbor PZT rods in calculating the strain profile

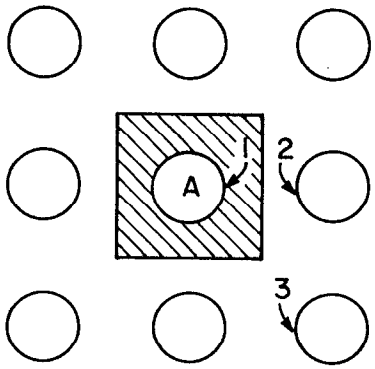

FIG. 8. Top view of a 1–3 composite. The area enclosed by the square is the unit cell and the circles are PZT rods. To calculate the polymer strain in the hatched area, only the nine PZT rods shown in the figure need to be considered if the ceramic content is less than 20%.

of the polymer phase in the hatched area of Fig. 8. Based on this consideration, the strain profile in the polymer phase of the unit cell can be approximated as

$$\left(\frac{2u}{L}\right)=A_0\sum_{n=1}^{9}K_0\left(\frac{|\mathbf{r}-\mathbf{r}_n|}{\xi}\right), \tag{3.1}$$

where the summation is over the nine PZT rods shown in Fig. 8 and $\mathbf{r}_i$ is the center position of the ith rod. A_0 is the normalization factor, which will be determined from the boundary conditions that the strain at the polymer–PZT rod interface is equal to that of the PZT rod and all the PZT rods have the same strain level. It is clear that Eq. (3.1) cannot meet these conditions and A_0 determined from different boundary points will be different. However, it can be shown that even for a composite containing 20% PZT, the variation of A_0 calculated from different boundary points is less than 10%. Within this error, Eq. (3.1) can be used to describe the strain profile of the polymer phase in the unit cell containing the PZT rod A. To account for the variation of A_0 at a different boundary point, A_0 is calculated at points 1, 2, and 3 of the PZT–polymer boundary. This gives three different A_0 and the final value of A_0 is the averaged one over these three values,

$$A_0=\left(\frac{1}{3}\right)\left(\frac{2u}{L}\right)_0\left(\frac{1}{L_1}+\frac{1}{L_2}+\frac{1}{L_3}\right), \tag{3.2}$$

where $(2u/L)_0$ is the strain of the PZT rod and $L_i=\Sigma_{n=1}^{9}K_0(|\mathbf{a}_i-\mathbf{r}_n|/\xi)$, $\mathbf{a}_i$ is the coordinate vector of the point labeled i in Fig. 8. From the results in Sec. III, d_{33} and d_h for the composite are, respectively,

$$d_{33}=v_0[1+A(a,\xi)]/[(1+{}^cs_{33}Y)A(a,\xi)]\,{}^cd_{33}, \tag{3.3}$$

$$d_h=\left[{}^cd_{33}\left(1+(1-2\sigma)A(a,\xi)-\frac{Y[{}^cs_h+(1-2\sigma)\,{}^cs_{33}A(a,\xi)]A(a,\xi)}{1+{}^cs_{33}YA(a,\xi)}\right)+2\,{}^cd_{31}\right]v_0, \tag{3.4}$$

the meaning of each quantity is the same as that in Eq. (2.14), except $A(a,\xi)$, which is defined as

$$A(a,\xi)=\frac{A_0}{\pi a^2}\sum_{n=1}^{9}\int_A K_0(|\mathbf{r}_n-\mathbf{r}|)\,dx\,dy, \tag{3.5}$$

where the integration is over the hatched area in Fig. 8. By assuming the strain in the polymer phase a constant, the above equations can be reduced to that derived earlier using the equal-strain approximation.[14]

Here d_h is calculated for 1–3 composites made of PZT-5A and spurs epoxy using Eq. (3.4). The parameters used in the calculation are obtained from the available literature.[15] For a 1–3 composite with 10% PZT volume content and the rod radius $a=0.3$ mm, the d_h values calculated are 55, 35, and 20 pC/N, respectively, for a sample thickness of $L=4$, 2, and 1 mm. These numbers are comparable with the experimental values: 61, 32, 17 pC/N measured by Klicker for composites with the corresponding material parameters.[8] For the composites with a higher volume fraction of PZT, the agreement between the theory and experiment becomes less satisfactory. This is what is expected from the assumption of this model.

V. CONCLUSIONS

In this paper, using the force equilibrium condition an elastic model is introduced to describe the deformation of 1–3 type composites under different driving conditions. Based on this, the effects of PZT rod aspect ratio, polymer shear and Young's moduli, as well as the spacing between PZT rods on the elastic coupling between the two components and the performance of composites are analyzed quantitatively. The theoretical results are in good agreement with experimental observations. Furthermore, using a double beam ultradilatometer, the strain profiles of several composites with simple structures were measured and the results can be described quite well by the theoretical predicted profiles. It is also shown that the strain profile measured in this manner can be used to describe the deformation of composites under a uniaxial or hydrostatic pressure.

ACKNOWLEDGMENT

We wish to thank Dr. Wally Smith for the stimulating discussions.

[1] R. E. Newnham, D. P. Skinner, and L. E. Cross, Mat. Res. Bull. **13**, 525 (1978).
[2] R. E. Newnham, L. J. Bowen, K. A. Klicker, and L. E. Cross, Mat. Eng. **2**, 93 (1980).
[3] T. R. Gururaja, A. Safari, R. E. Newnham, and L. E. Cross, in *Electronic Ceramics*, edited by L. M. Levinson (Marcel Dekker, New York, 1987), Vol. 92.
[4] W. A. Smith and B. A. Auld, IEEE Trans. Ultrason. Ferroelectrics., Freq. Controls **38**, 40 (1991).
[5] W. A. Smith and A. A. Shaulov, Ferroelectrics **87**, 309 (1988).
[6] G. Hayward and J. A. Hossack, J Acoust. Soc. Am. **88**, 599 (1990).
[7] B. A. Auld, H. A. Kunkel, Y. A. Shui, and Y. Wang, Proc. 1983 IEEE Ultrason. Symp. 554 (1983).
[8] K. A. Klicker, Ph.D. thesis, The Pennsylvania State University, 1980.
[9] W. A. Smith, Proc. 1990 IEEE Ultrason. Symp. 145 (1990).

[10] Q. M. Zhang, S. J. Jang, and L. E. Cross, J. Appl. Phys. **65**, 2808 (1989).
[11] W. Cao, Q. M. Zhang, and L. E. Cross, IEEE Trans. Ultrason. Ferroelectrics., Freq. Controls (in press).
[12] T. R. Gururaja, Ph.D. thesis, The Pennsylvania State University, 1984.
[13] The d_h values measured on the samples provided by FMI, Maine.
[14] M. J. Haun and R. E. Newnham, Ferroelectrics **68**, 123 (1986).
[15] In the calculation, $\sigma=\frac{1}{3}$ for the polymer phase and ${}^{c}s_{12}=\frac{1}{3}{}^{c}s_{33}$ for PZT rods are assumed; other parameters used in the calculation are from the data sheet of Morgan Matroc. Inc. and Refs. 8 and 12.